Intrinsically Microporous Polymer Nanosheets for High-Performance Gas Separation Membranes

Supporting Information

for *Macromol. Rapid Commun.*, DOI: 10.1002/marc.201900572

Intrinsically Microporous Polymer Nanosheets for High-Performance Gas Separation Membranes

Marzieh Tamaddondar, Andrew B. Foster, Jose M. Luque-Alled, Kadhum J. Msayib, Mariolino Carta, Sara Sorribas, Patricia Gorgojo, Neil B. McKeown, and Peter M. Budd*

Supporting Information

Intrinsically Microporous Polymer Nanosheets for High Performance Gas Separation Membranes

Marzieh Tamaddondar, Andrew B. Foster, Jose M. Luque-Alled, Kadhum J. Msayib,

*Mariolino Carta, Sara Sorribas, Patricia Gorgojo, Neil B. McKeown & Peter M. Budd**

Dr Marzieh Tamaddondar, Dr Andrew B. Foster, Dr Sara Sorribas and Prof. Peter M. Budd
Department of Chemistry, University of Manchester, M13 9PL, Manchester, UK
Email: Peter.Budd@manchester.ac.uk

Jose M. Luque-Alled, Dr Patricia Gorgojo
Department of Chemical Engineering and Analytical Science,
University of Manchester, M13 9PL, Manchester, UK

Dr Kadhum J. Msayib and Prof. Neil B. McKeown
EastChem, School of Chemistry, University of Edinburgh,
David Brewster Road, EH9 3FJ, Edinburgh, UK

Dr Mariolino Carta
Department of Chemistry, College of Science, Swansea University,
Grove Building, Singleton Park, SA2 8PP, Swansea, UK

CONTENTS

Page

1. Materials

5,5′,6,6′-Tetrahydroxy-3,3,3′,3′-tetramethyl-1,1′-spirobisindane (TTSBI, 98%) was purchased from Alfa Aesar and was purified as follows: TTSBI (20 g) was dissolved in hot methanol (400 ml, 120 °C), re-precipitated from dichloromethane (DCM, 250 ml) and dried in a vacuum oven at 50 °C for 5 h before use. Tetrafluoroterephthalonitrile (TFTPN, 98%) was purchased from Sigma-Aldrich and was used without purification. Anhydrous potassium carbonate (K_2CO_3, 99.0%), purchased from Fisher, was finely ground and oven-dried at 100°C overnight before being used. Hexaethylphosphorous triamide (97 %) and pentafluorobenzonitrile (99%), used to synthesize 4,4′-dicyano- 2,2′,3,3′,5,5′,6,6′-octafluorobiphenyl monomer, were purchased from Sigma-Aldrich. Anhydrous N,N-dimethylacetamide (DMAc, 99.8%), anhydrous N,N-dimethylformamide (DMF, 99.8 %), anhydrous dichlorobenzene (DCB, 99%), anhydrous chloroform ($CHCl_3$, 99%), research grade $CHCl_3$ (≥ 99.5%), methanol, acetone, anhydrous 1,4-dioxane, tetrahydrofuran (THF, ≥99.9%), anhydrous diethyl ether (50 ppm water) and anhydrous DCM were purchased from Sigma Aldrich.

2. PIM-1 synthesis

A clean 250 ml three-neck, round bottom flask was dried overnight at 100 °C. 5,5',6,6'-tetrahydroxy-3,3,3',3'-tetramethyl-1,1'-spirobisindane, TTSBI (10.212 g, 0.03 mol), tetrafluoroterephthalonitrile, TFTPN (6.003 g, 0.03 mol) and anhydrous potassium carbonate (12.483 g, 0.09 mol) were added to the flask and the solid mixture was mechanically stirred for 30 min at room temperature under a flow of dry nitrogen. Anhydrous dimethylacetamide (DMAc, 60 ml) and anhydrous dichlorobenzene (DCB, 30 ml) were added to the mixture and the mixture was stirred again for another 30 min under N_2 at room temperature to reach a homogeneous mixture. At this point the temperature of the heater was set to 160 °C and the

flask was equipped with a Dean-Stark trap to condense and collect the produced water from the reaction mixture. The reaction was completed in a total of 40 min (18 min was required for the heater to reach the set temperature of 160 °C). At the end of the reaction, the highly viscous solution was poured into methanol (300 ml) while still hot and was filtered. The dried reaction product was dissolved in chloroform (300 ml), re-precipitated from methanol (900 ml) and then washed with deionized water under reflux at 95 °C overnight. Purification and solvent extraction was continued by washing the polymer with 1,4 dioxane (200 ml), acetone (400 ml) and two times methanol (300 ml each time). Finally, the purified PIM-1 was dried in a vacuum oven at 120 °C overnight to obtain 12.66 g of PIM-1 (yield: 91%). 10 mg of the polymer was dissolved in 10 ml of filtered chloroform to prepare 1 mg ml^{-1} of polymer solution and then the solution was filtered using a 0.45 micron PTFE syringe filter. The polymer was tested for molecular weight distribution using a multi detector GPC and the results (see **Figure S1**) showed M_w = 158,000 g mol^{-1}, PDI= 2.95. ^{1}H NMR (400 MHz, $CDCl_3$, δ, ppm): 6.82 (2H, s), 6.43(2H, s), 2.34−2.16 (4H, dd), 1.48−1.11 (broad, 12H). ATR-IR (cm^{-1}): 2995, 2864, 2239, 1605, 1446, 1264. Anal. Calc. for $C_{29}H_{20}N_2O_4$ (wt. %): C, 75.64; H, 4.37; N, 6.08, Found: C, 74.20; H, 4.10; N, 5.8.

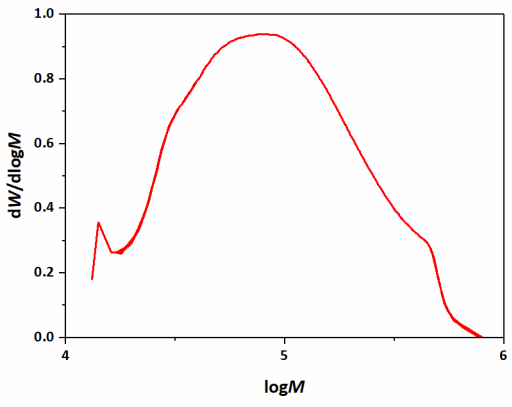

Figure S1. Molecular weight distribution of PIM-1 obtained from multi detector GPC

3. Synthesis of 4,4'-dicyano-2,2',3,3',5,5',6,6'-octafluorobiphenyl

A homogenous solution of pentafluorobenzonitrile (10.0 g, 51.8 mmol) in anhydrous diethyl ether (30 ml) was prepared and hexaethylphosphorous triamide (6.40 g, 25.9 mmol) was added to it drop by drop. In order to avoid the evaporation of the solvent during this exothermic reaction, the mixture was kept in an ice bath under a very gentle flow of dry nitrogen throughout the addition. After this step, the reaction was slowly returned to room temperature while being stirred under a very gentle flow of N_2 for 3 h. The reaction was stopped and the mixture was concentrated under reduced pressure at room temperature. The crude reaction products were then dried overnight at room temperature and were purified by column chromatography (hexane/DCM, 3/3) to give the main product, 4,4'-dicyano-2,2',3,3',5,5',6,6'- octafluorobiphenyl (3.02 g, yield 33%) as a white powder. ATR-IR (cm^{-1}) spectra, shown in **Figure S2**, 2247, 1481, 1287, 1268, 1003 cm^{-1}. ^{19}F NMR (400 MHz, $CDCl_3$) δ - 129.7 (m, 4F, ArF), - 133.5 (m, 4F, ArF) [lit. ^{19}F NMR ($CDCl_3$) δ - 129.8 (4F), - 133.7 (4F)][1]; ^{13}C NMR (400 MHz,$CDCl_3$) δ 148.5 (m), 145.9 (m), 145.3 (m), 142.7 (m) 111.7 (m), 106.5, 97.3 (m) (^{19}F- ^{13}C coupling not assigned).

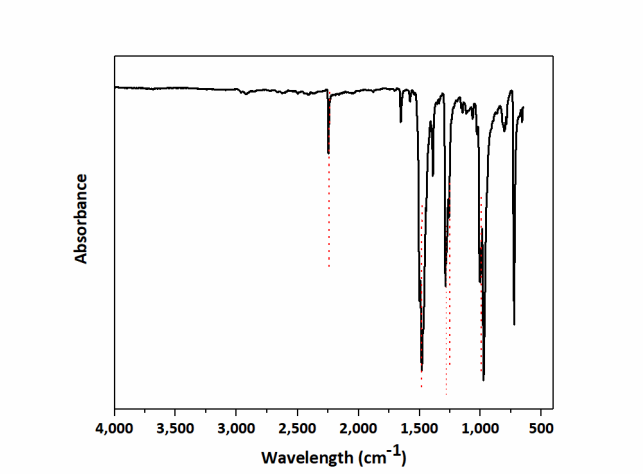

Figure S1. IR spectra of 4,4'-dicyano- 2,2',3,3',5,5',6,6'- octafluorobiphenyl

4. Characterization of network-PIM-1

Elemental analysis of the network PIM-1: Calc. for $C_{56}H_{40}N_2O_8$ which assumes a fully reacted network structure (wt. %): C, 77.40; H, 4.65; N, 3.22, Found: C, 71.04; H, 4.64; N, 3.38; F, 2.25. The carbon / nitrogen ratio and significant fluorine content of the network PIM-1 sample suggests that a typical fragment of the network structure is along the lines presented in **Figure 1b** of the manuscript.

A 3D representation of the network PIM-1 structure was constructed using a Molymod molecular model building kit. Equal numbers of both stereoisomers of the spiro monomer unit were incorporated into the final large scale structure. An example of four spiro units attached around a single biphenyl unit [central unit, with nitrogen atom (blue) of top CN visible] is presented in **Figure S3**. Two of each type of stereoisomer are included in this open structure, identified from each other by whether the oxygen (red) atoms depicted in the structure contain open (A) or filled in (B) holes.

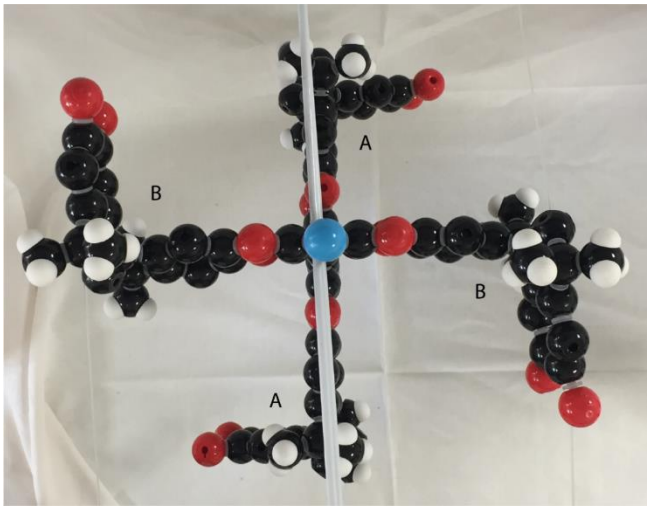

Figure S3. Example of a fully reacted biphenyl unit. This open arrangement represents only one of a number of ways in which spiro stereoisomers can be arranged around the central biphenyl unit.

It was clearly evident from building up the 3D structure further, with more biphenyl units, that not all reactive sites [pairs of fluorine (green) atoms] on each consecutive biphenyl unit were able to fully react as the network structure expanded, owing to steric constraints within the growing network structure, presented in **Figure S4**.

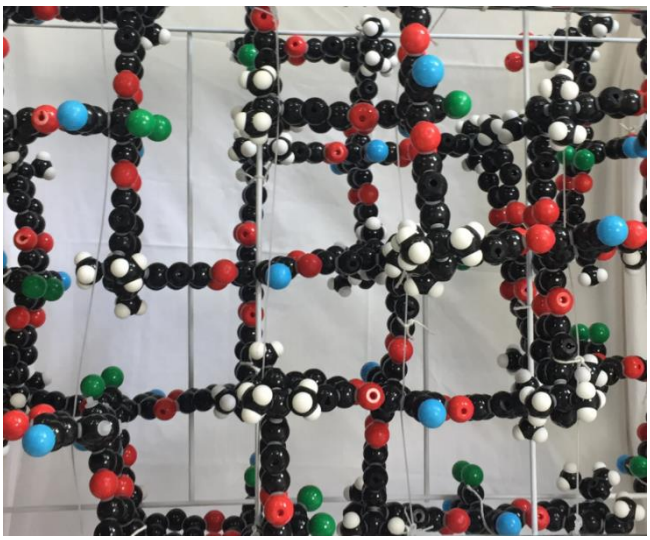

Figure S4. Representation of the extended PIM-1 network structure, which includes a mixture of arrangements of the spiro stereoisomers around each biphenyl unit.

In the larger irregular representation of the PIM-1 network (**Figure S4**), it can clearly be seen that when further network growth occurs the incorporated biphenyl units are all still arranged perpendicular to the plane of the image [only nitrogen (blue) atoms on the top CN groups of the structure are clearly evident in this image]. Whereas the growth perpendicular to the plane of the image is limited to a couple of layers of atoms (3-5 nm), the nature of how the spiro units link to the consecutive biphenyl units means that the vast majority of reactive groups in the developing structure are generated around the edges of the extended plane of the image. The amount of free unreacted fluorine atoms depicted in this network structure broadly reflects the amount of fluorine determined in the elemental analysis of the network sample. The physical 3D modelling structures developed do suggest the feasibility of nanosheet formation, with a high aspect ratio, starting from combination of these two monomers.

Solid-state ^{13}C NMR was used to characterize both network-PIM-1 and PIM-1 and the results indicated the same chemical shifts for both polymers, as shown in **Figure S5**. Solid state NMR of network PIM-1 is almost indistinguishable from that of PIM-1. Signals are usually broad in this analysis and not really amenable for looking quantitatively for subtle structural differences. The likely signals due to aromatic carbons attached to F also fall in the same resonance region (140-150 ppm) as other signals. An overall broadening of the signal in this region would suggest that there are free fluorines present in the structure, as the elemental analysis suggests.

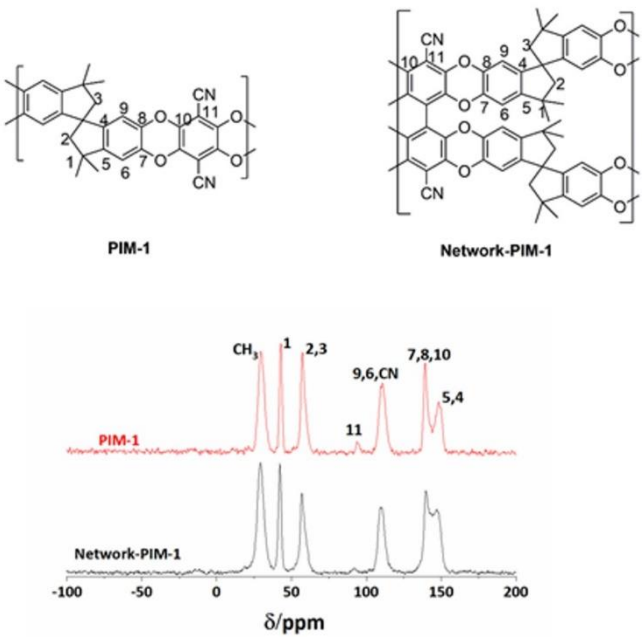

Figure S5. Solid ^{13}C NMR spectra (400 MHz) showing chemical shifts of network-PIM-1 compared to PIM-1

FTIR spectra of network-PIM-1 and PIM-1 are shown in **Figure S6**. It can be observed from this figure that network-PIM-1, similar to PIM-1, has an absorbance peak at 1446 cm^{-1} which is related to C-O groups in benzodioxane rings in the polymer network. FTIR (cm^{-1}): 2995, 2864, 2239, 1605, 1446, 1264.

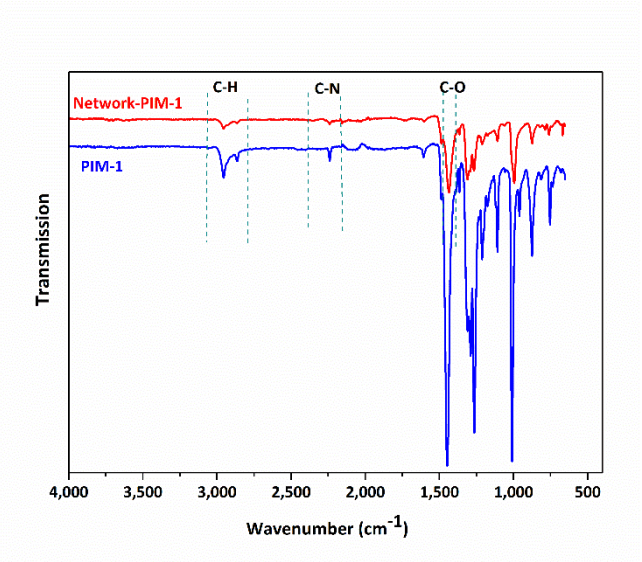

Figure S6. FTIR spectra of network-PIM-1 compared to PIM-1

Shown in **Figure S7** are the results obtained from SEM analysis of network-PIM-1 spray coated from a chloroform-based dispersion onto a silicon wafer.

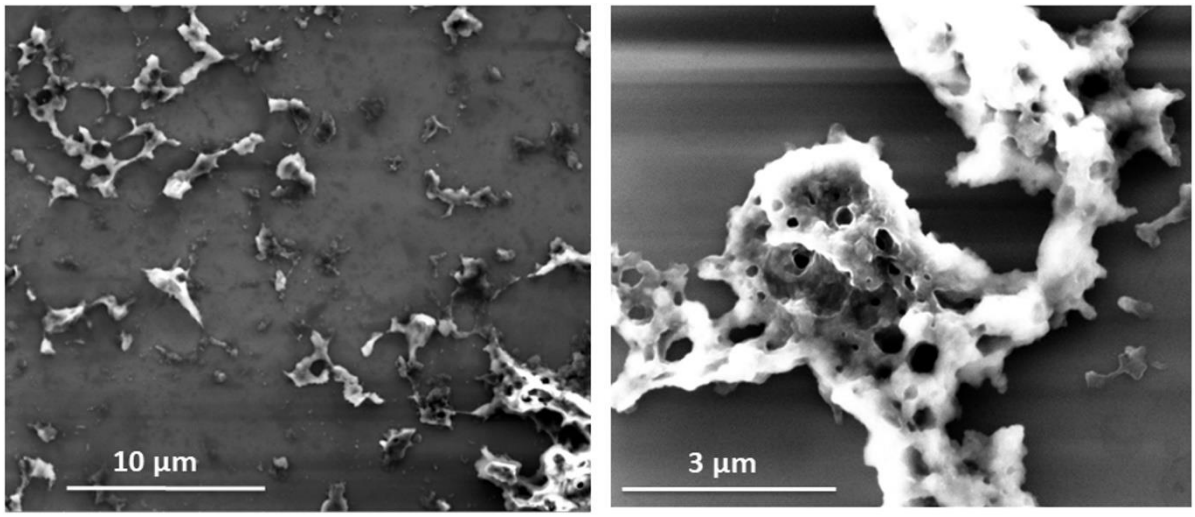

Figure S7. SEM images taken from spray coated dispersion of network-PIM-1 in chloroform on silicone wafer

Elemental mapping for C, N, O, F, K and Cu by Energy Dispersive X-ray Spectroscopy (EDX) for a sheet-like structure in a STEM image is shown in **Figure S8**. These maps confirm the presence of an organic sheet-like morphology.

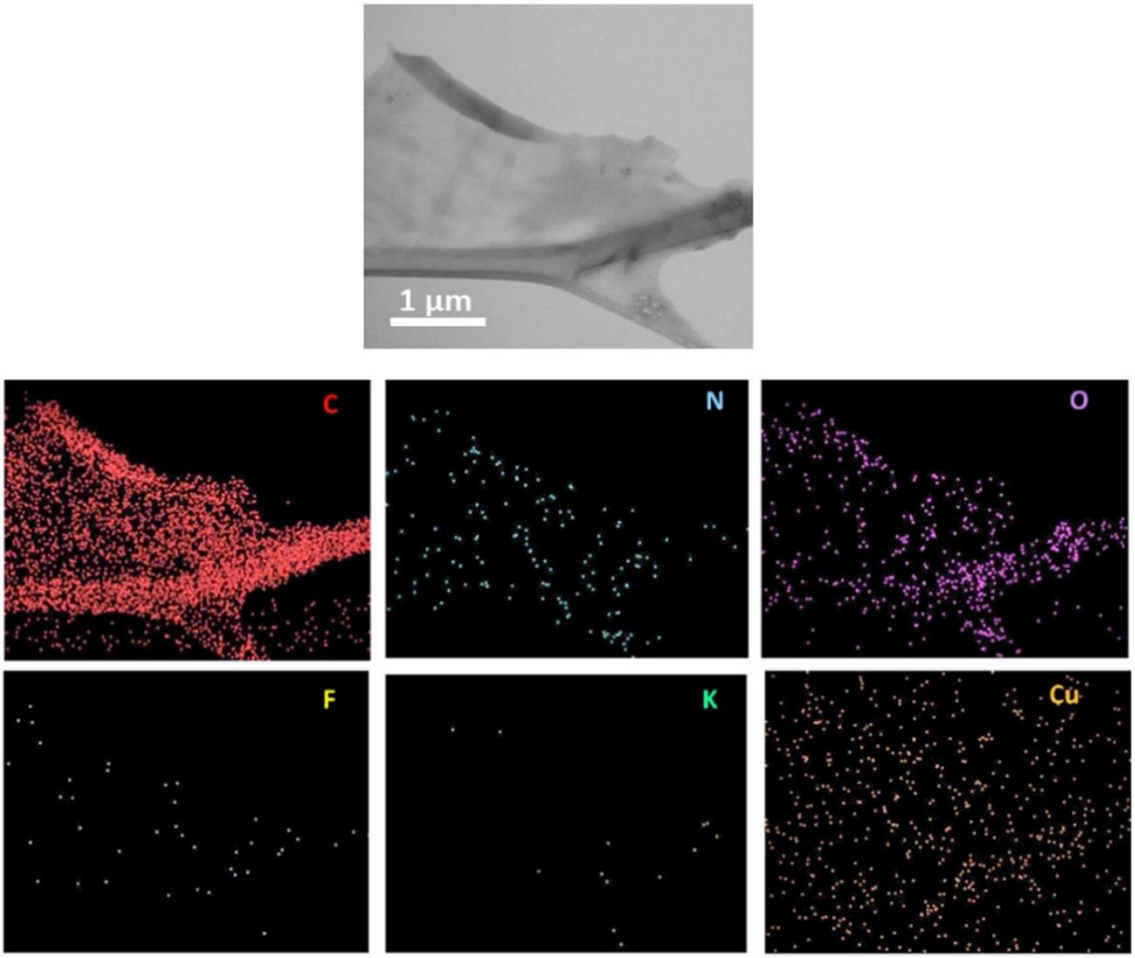

Figure S8 Bright field STEM image and the respective elemental mapping results for C, N, O, F, K and Cu

X-ray diffraction (XRD) paterns of network-PIM-1 and PIM-1 powder are shown in **Figure S9.**

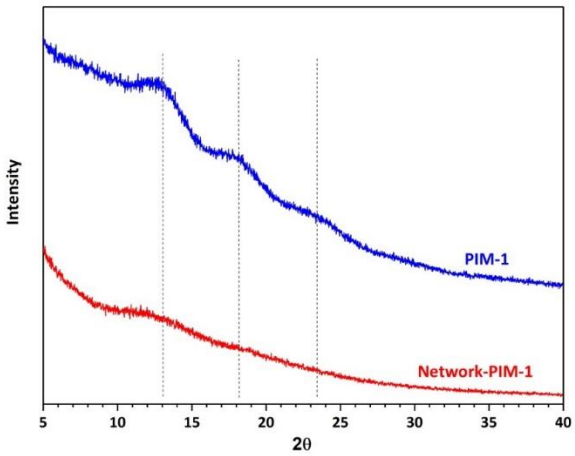

Figure S9. X-ray scattering data for network-PIM-1 compared to PIM-1 powder

5. Morphology of mixed matrix membranes

Changes in the morphology of mixed matrix membranes (MMMs) upon addition of different contents of network-PIM-1 can be seen in the SEM images shown in **Figure S10a** to **Figure S10c.** Agglomeration of network-PIM-1 particles at higher conecntrations of the filler can be seen **Figure S10b** and **Figure S10c** related to 5 wt.% and 10 wt.% loading of network-PIM-1, respectively.

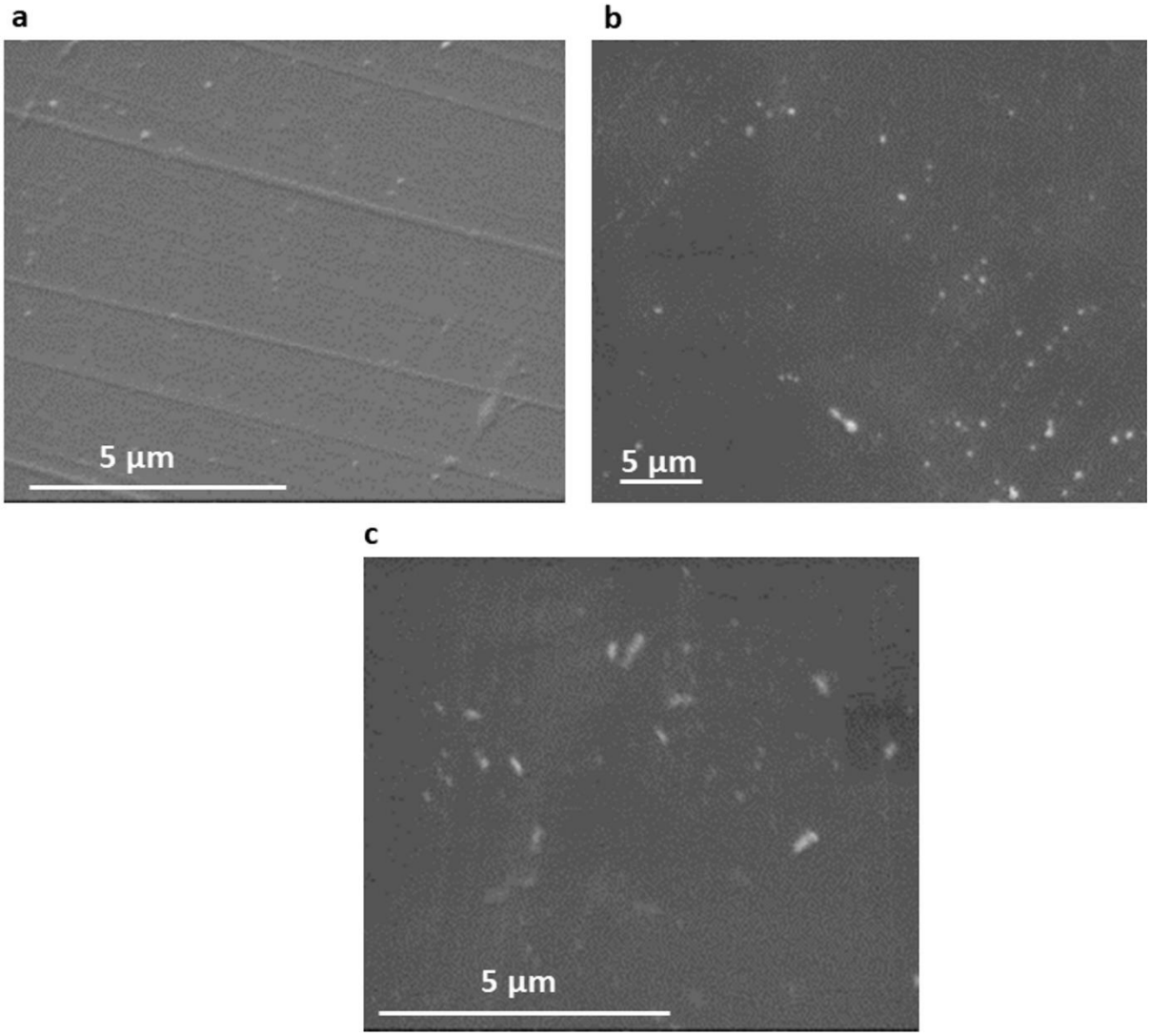

Figure S10. Surface SEM images of MMMs with **a** 0.027 wt.%, **b** 5 wt.% and **c** 10 wt.% of network-PIM-1 in PIM-1

Images from polarized light microscopy of an MMM with higher loading of network-PIM-1 (20 wt.%) in PIM-1 are shown in **Figure S11**.

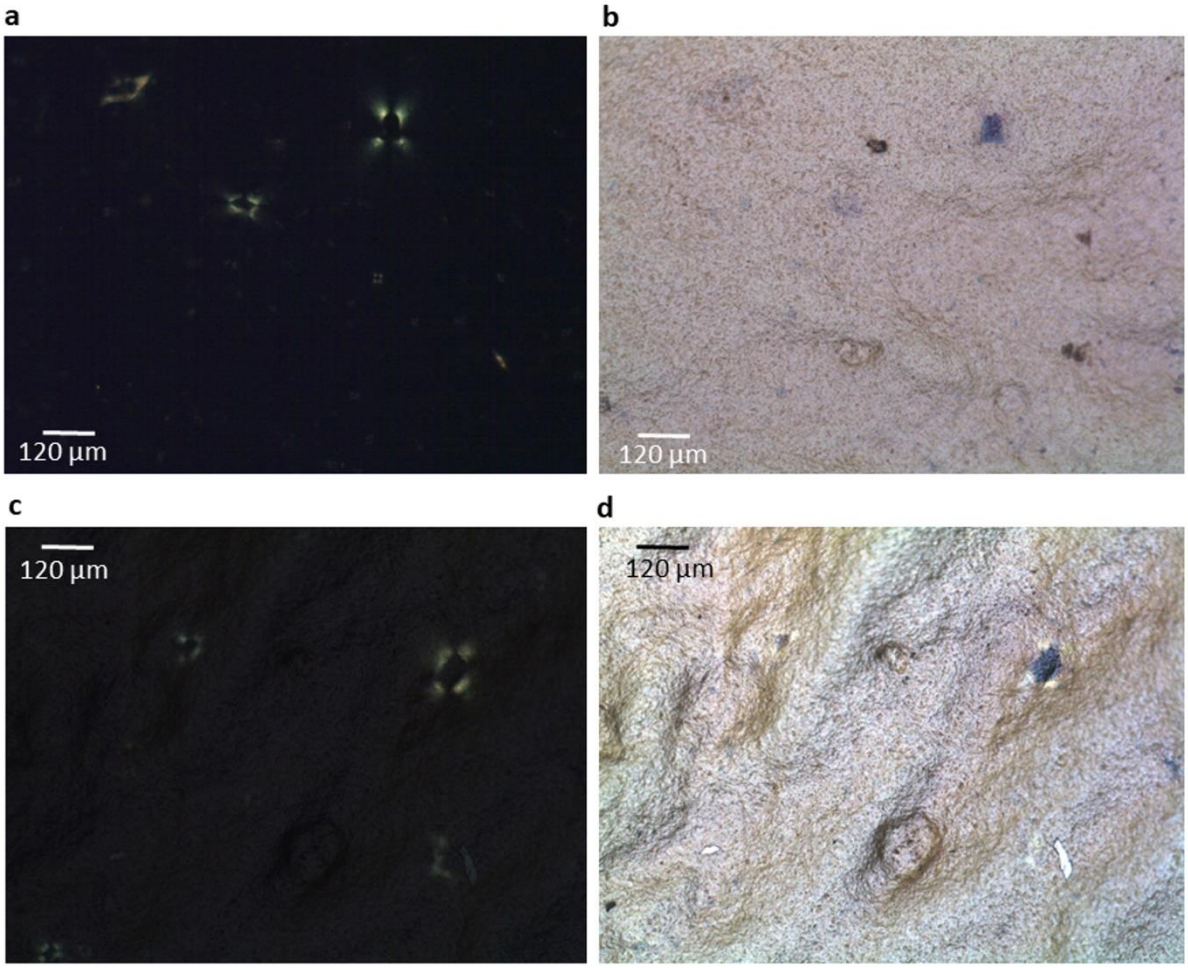

Figure S11. Polarized light microscopy of a membrane with 20 wt.% network-PIM-1 in PIM-1 (thickness 89 µm). **a, c** Membrane between crossed polars showing birefringence of filler particles. **b, d** Corresponding images to a and c with parallel polars.

6. Mixed gas separation performance

Mixed gas permeation data for both as-cast and methanol-treated MMMs containing five different loadings of network-PIM-1 (0.027, 0.2, 0.5, 5, 10 wt.% with respect to the total solid) are summarized in **Table S1** and **Table S2**, respectively.

Table S1. CO_2/CH_4 mixed-gas (1:1, v:v) separation performance of the as-cast PIM-1 and MMMs; measurements were done at transmembrane pressure difference of 2 bar and 25 °C

Membrane	***P*** $_{CO2}$ **(Barrer)**	**CO_2/CH_4 selectivity**	**Thickness (μm)**
PIM-1	2100 ±280	12.7 ±0.3	64±8
MMM-0.027 wt.%	4676 ±110	16.1 ±0.6	63±4
MMM-0.2 wt.%	8070 ±700	10.8 ±0.5	57±6
MMM-0.5 wt.%	6470 ±340	13.3 ±0.4	60±8
MMM-5 wt.%	4060 ±450	16.5 ±1.2	64±2
MMM-10 wt.%	3700 ±320	18.5 ±0.5	67±3

Table S2. CO_2/CH_4 mixed-gas (1:1, v:v) separation performance of the MeOH-treated PIM-1 and MMMs; measurements were done at transmembrane pressure difference of 2 bar and 25 °C

Membrane	***P*** **$_{CO2}$** **(Barrer)**	**CO_2/CH_4 selectivity**	**Thickness (μm)**
PIM-1	5917 ±380	13.1 ±0.44	59±10
MMM-0.027 wt.%	5371 ±440	13.7 ±0.64	67±4
MMM-0.2 wt.%	5160 ±190	11.2 ±1.5	63±4
MMM-0.5 wt.%	9778 ±527	14.4 ±0.7	67±10
MMM-5 wt.%	5218 ±600	14.1 ±0.7	66±3
MMM-10 wt.%	4600 ±300	21.5 ±1.5	80±3

[1] A. Alberola, R. Less, F. Palacio, C. Pask, J. Rawson, *Molecules.* **2004**, *9*, 771.